

An Estimation of the Coupling Coefficient of the Series Inductive Resonant Wireless Power Transfer Coils

I. Adam^{1,2}, Sheroz. Khan¹, Z. Zaharudin^{1,2}, K. Abdul Kadir², A. N. Nurdin¹, M. Yaacob¹

¹Kulliyah of Engineering, International Islamic University, P. O. Box 10, 50728 Kuala Lumpur, Malaysia

²University of Kuala Lumpur, British Malaysian Institute, Batu 8, Jalan Sungai Pusu, 50728 Kuala Lumpur, Malaysia

¹i.adam.mlk@gmail.com

Article Info

Volume 81

Page Number: 5756 - 5761

Publication Issue:

November-December 2019

Abstract

Though the power transfer efficiency of the inductive resonant wireless power transfer is relatively high, the power transfer efficiency of the inductive resonant wireless power transfer is undoubtedly depending on the coupling coefficient. Coupled with the coupling coefficient, the highest possible power transfer efficiency can be achieved by controlling the operating frequency with impedance matching. Therefore, the relationship of the input impedance to the variation of the coupling coefficient is of paramount importance in maintaining the highest possible power transfer efficiency for a given coupling coefficient. This paper presents the relationship of the input impedance of the series-to-series inductive resonant wireless power transfer to the variations of the coupling coefficient. The analysis is carried out by using the T-equivalent circuit, producing analytical results for comparison and validation by equivalently obtained simulation results, guarantying the maximum power transfer efficiency for a typical series-to-series inductive resonant link. The modeling validity is shown by percentage error in between the analytical and simulation results. The novelty of this paper is in the simplicity of the coupling coefficient estimation by reference to the input impedance.

Keywords: Input Impedance; T-equivalent Circuit; Coupling Coefficient Estimation

Article History

Article Received: 5 March 2019

Revised: 18 May 2019

Accepted: 24 September 2019

Publication: 27 December 2019

1. Introduction

Wireless power transfer (WPT) is a technology of transferring energy to a load at a distance without physical contact. The technology has gained popularity especially in the application requiring no physical contact, ensuring thus safety and convenience of usage. For instance, the wireless power transfer has been used for powering medical implants and for applications such as in the remote charging of batteries, powering of implantable-cardioverter- defibrillator [1-2]. In the automotive industry, wireless power transfer is used in the charging of electric vehicles [3].

Historically, wireless power transfer technology is invented and experimented by Nicolas Tesla in the late

19th century. In 2007, the group of researchers from Massachusetts Institute of Technology (MIT) hit the breakthrough of the wireless power transfer technology by successfully transmitting power over a distance of two meters achieving an efficiency of 40% [4]. Though not used for years after its first Tesla experiment, suddenly, the research in the area of wireless power transfer has rejuvenated so wildly popular these days for applications not imagined years ago.

The following categories have been generally used to describe wireless power transfer technology such as radiative, non-radiative capacitive coupling and non-radiative magnetic coupling. The radiative wireless power transfer technology such as microwave or laser usually used to transfer high power. Also, in transferring power,

the radiative wireless power transfer technology uses electromagnetic radiation for far-field transmission. However, due to its omnidirectional character; the efficiency is very low makes this technology most suitable for transmitting information. Besides, the microwave and laser are unsafe to human beings and livestock alike. However, in practice, microwave and laser have been used for charging of the drone energy storage devices from satellite, out of human beings vicinity. While the non-radiative capacitive coupling wireless power transfer technology uses an electric field from a capacitive coupling for near-field transmission. The non-radiative capacitive coupling wireless power transfer technology requires high voltages in transferring of high power, more sensitive and complex for wireless power harvesting system. The huge voltage generated in transferring high power and alongside the resulting electric field harms the human body [5]. Due to these reasons, the non-radiative capacitive coupling wireless power transfer technique which was the main scheme of wireless power transfer in the early days of wireless power transfer is less preferred in the recent wireless power transfer works. Whereas the non-radiative magnetic coupling wireless power transfer system uses a near-field transmission technology which is a magnetic field in transferring power. With the inclusion of a tuned capacitor, the technology can transfer a great deal of power at a longer distance [6]. The inductive resonant wireless power transfer has become the premier area in wireless power transfer research recently. Additionally, the nature of comfortable implementation [7] of inductive resonant wireless power transfer coupling makes the inductive resonant wireless power transfer technique the first choice. In [8], the power transfer distance and efficiency are reposted can be improved by adopting the resonance principle-based inductively coupled coils in the system.

At a present, a lot of wireless power transfer research study is focusing on distance coverage and power efficiency [9-10]. Several methods such as impedance matching; it has been proposed to maximize the efficiency of the wireless power transfer system. However, most of them require the knowledge of systems parameters such as the coupling coefficient to maximize the power transfer [10-12]. In [6], we have shown that the coupling coefficient governs the power transfer efficiency of the wireless power transfer. While in [13-14], the maximum power transfer efficiency is tackled by considering the coupling coefficient variation. Consequently, the coupling coefficient estimation is a crucial factor to make efficient wireless power transfer implementation. This paper presents derivations of equations for estimation of coupling coefficients in the series-to-series inductive resonant wireless power transfer system. Through the MATLAB simulation, this study confirms that the coupling coefficient estimation can be made possible by monitoring the voltage and current of the transmitting side.

1.1 The T-Equivalent Circuit of the Magnetically Coupled Circuit

In [3], we have discussed the conversion of the magnetically coupled circuit to the T-equivalent circuit in detail. Despite that, in this paper, the conversion is lightly revisited to give an insight idea of the theoretical background of the series-to-series WPT magnetically coupled circuit conversion into its T-equivalent circuit.

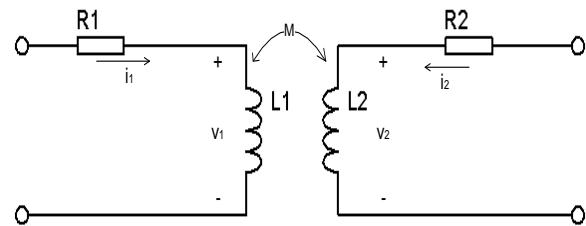


Figure 1: Magnetically coupled circuit

From Figure 1, the input and output terminal voltages can be written as in.

$$v_1 = L_1 \frac{di_1}{dt} + M \frac{di_2}{dt} \quad (1)$$

$$v_2 = M \frac{di_1}{dt} + L_2 \frac{di_2}{dt} \quad (2)$$

Therefore, the magnetically coupled circuit in Figure 1 can be easily converted into its T-equivalent circuit as in Figure 2, by using Equations (1) and (2).

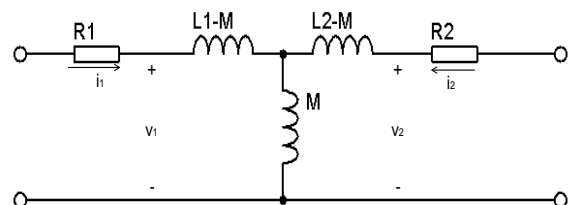


Figure 2: The general T-equivalent circuit of the magnetically coupled circuit

In a study of the inductive resonant WPT, the T-equivalent circuit model as shown in Figure 2 is widely used due to the simplicity it provides to analyze the wireless power transfer topology. Likewise, this is the reason the T-equivalent circuit is used in this paper.

1.2 The Input Impedance of the Series-To-Series WPT

The T-equivalent circuit of the series-to-series WPT topology as shown in Figure 3 is formed by adding the voltage source (V_s) and primary capacitor (C_1) at the front end of the general T-equivalent model of Figure 2. While at the back end of the general T-equivalent is added with the load resistance (RL) and secondary capacitor (C_2) as shown in Figure 3.

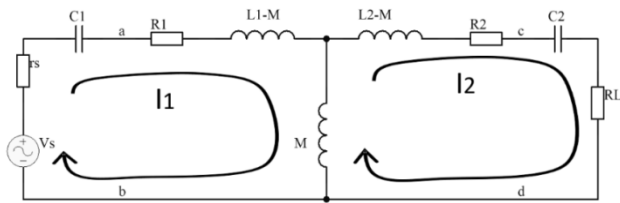


Figure 3: The T-equivalent circuit of the series-to-series WPT topology

In matrix form, the equations which relate the input and output of the series-to-series WPT topology as shown in Figure 3 can be written as follows

$$\begin{bmatrix} V_S \\ 0 \end{bmatrix} = \begin{bmatrix} rs + R_1 - j\frac{1}{\omega C_1} + j\omega L_1 & -j\omega M \\ -j\omega M & R_2 + R_L + j\omega L_2 - j\frac{1}{\omega C_2} \end{bmatrix} \begin{bmatrix} I_1 \\ I_2 \end{bmatrix} \quad (3)$$

By letting $rs + R_1 - j\frac{1}{\omega C_1} + j\omega L_1$ is equal to z_{11} and $R_2 + R_L + j\omega L_2 - j\frac{1}{\omega C_2}$ is equal to z_{22} , Equation (3). can be simplified to

$$\begin{bmatrix} V_S \\ 0 \end{bmatrix} = \begin{bmatrix} z_{11} & -j\omega M \\ -j\omega M & z_{22} \end{bmatrix} \begin{bmatrix} I_1 \\ I_2 \end{bmatrix} \quad (4)$$

The input current I_1 , and the output current I_2 can be deduced to Equations (5) and (6) by using Cramer's rules

$$I_1 = \frac{\Delta I_1}{\Delta} \quad (5)$$

$$I_2 = \frac{\Delta I_2}{\Delta} \quad (6)$$

Where Δ , ΔI_1 and ΔI_2 are $z_{11}z_{22} + \omega^2 M^2$, $V_S z_{22}$ and $j\omega M V_S$ respectively. Finally, the input impedance of the

series-to-series WPT topology shown in Figure 3 can be derived and written as

$$Z_{in} = \frac{V_S}{I_1} = \frac{z_{11}z_{22} + \omega^2 M^2}{z_{22}} = z_{11} + \frac{\omega^2 M^2}{z_{22}} \quad (7)$$

The coupling coefficient (k) can be included in the Equation (7) by replacing mutual inductance (M) with $k\sqrt{L_1 L_2}$. Equation (8) is used extensively to calculate the input impedance in this paper.

$$Z_{in} = z_{11} + \frac{\omega^2 [k\sqrt{L_1 L_2}]^2}{z_{22}} \quad (8)$$

2. Design of Experiment Setup

The MATLAB ® Simulink tool uses in the simulation of finding the relationship of input impedance and the coupling coefficient. Figure 4 shows the Simulink model mimics the series-to-series inductive resonant WPT circuit. The RMS input voltage and RMS input current were monitored to yield the input impedance of the system. In general, the division of RMS voltage and RMS current makes the input impedance of the WPT. The ac signal is set to 1V peak-to-peak at a resonance frequency of 1590 Hz. Similarly, all other measurements are set to 1590 Hz. The simulation is conducted by setting the coupling coefficient to vary in steps as listed in column 1 of Table 1. For all the established coupling coefficient; the corresponding measured input impedances are copied into column 2 of Table 1. The source impedance (r_s), primary coil resistance (R_p), secondary coil resistance (R_s) is set to 1Ω while the load resistance (load) is set to 100Ω . To complete the circuit, the primary capacitance (C_p) and secondary capacitance (C_s) is set to $1\mu F$ and the primary and secondary inductance is set to $10mH$.

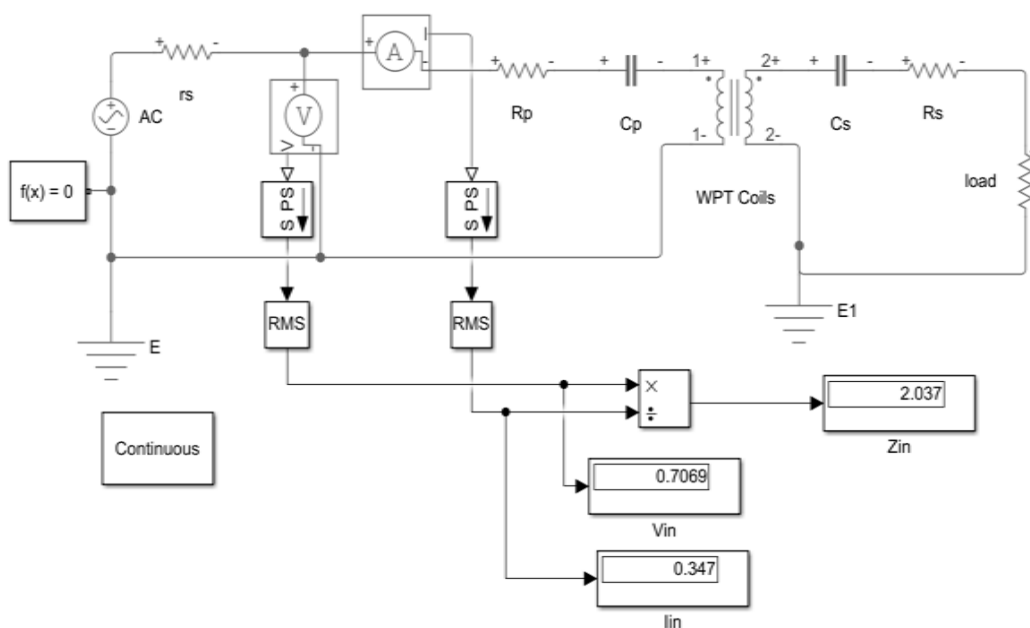


Figure 4: The MATLAB ® Simulink circuit

For the comparison, the input impedance calculation is achieved by designing the MATLAB ® m file using Equation (8). The calculation is carried out by frequency sweeping from 500 Hz to 5000 Hz in the step of 10 Hz, for all values of the coupling coefficient (k). In each iteration, the calculated input impedance at the resonance frequency is copied. Further, the calculated input impedance is listed in column 2 of Table 1. The resonant frequency (F_r) of the circuit can be calculated by Equation (9).

$$F_r = \frac{1}{2\pi\sqrt{L_x C_x}} \quad (9)$$

In this paper, the value of L_x and C_x are the inductance and capacitance of the primary and the secondary circuits.

3. Results and Discussion

The calculated and simulated input impedance with respect to the coupling coefficient (k) is listed in Table 1. As expected, the input impedance either by calculation or simulation showing incremental trends by incrementing of the coupling coefficient.

Table 1: Input impedance against the coupling coefficient

Coupling Coefficient (k)	Input Impedance	
	Simulation	Calculation
0.01	2.037	2.019
0.10	3.012	2.994
0.20	5.973	5.956
0.30	10.910	10.895
0.40	17.840	17.812
0.50	26.740	26.705
0.60	37.610	37.574
0.70	50.460	50.420
0.80	65.280	65.243
0.90	82.050	82.050
0.99	98.850	98.850

The plot of the calculated input impedance against the frequency is shown in Figure 5. The circuit frequency at which the minimum input impedance occurred is shifted to the left by the incrementing of the coupling coefficient (k). However, at the resonance frequency, the input impedance is incremented by the coupling frequency. The input impedance for all the respecting coupling coefficient is tabulated in column 2 of Table 1.

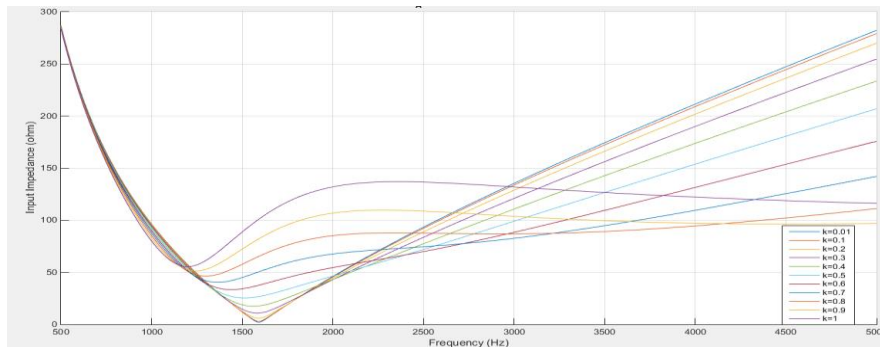


Figure 5: The plot of input impedance against frequency for coupling coefficient of 0.01, 0.1 to 1

Figure 6 shows the graph of the calculated input impedance against the coupling coefficient. The graph shows the almost linear increment of the input impedance

versus the coupling coefficient. The graph shows an almost linear relationship between the input impedance against the coupling coefficient.

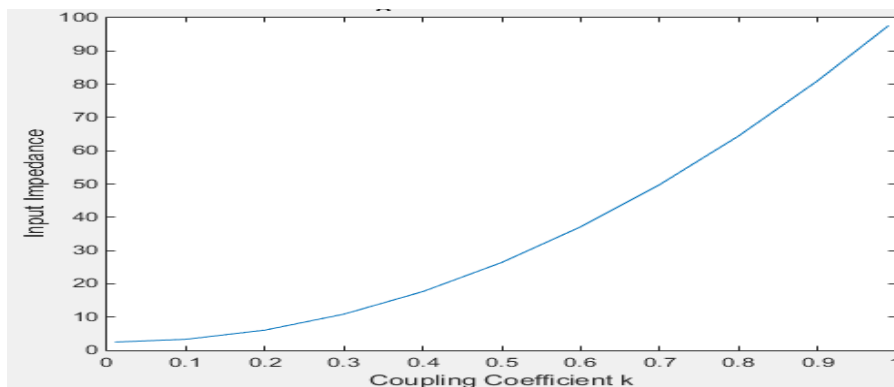


Figure 6: The graph of calculated input impedance against the coupling coefficient

To further investigate the relationship of the input impedance and the coupling coefficient of the series-to-series inductive resonant WPT, the calculated and simulated input impedance against the coupling coefficient is plotted in Figure 7. At a glimpse, both

graphs almost identical and similar. This indicates that the coupling coefficient of the series-to-series inductive resonant WPT can be estimated by using the input impedance.

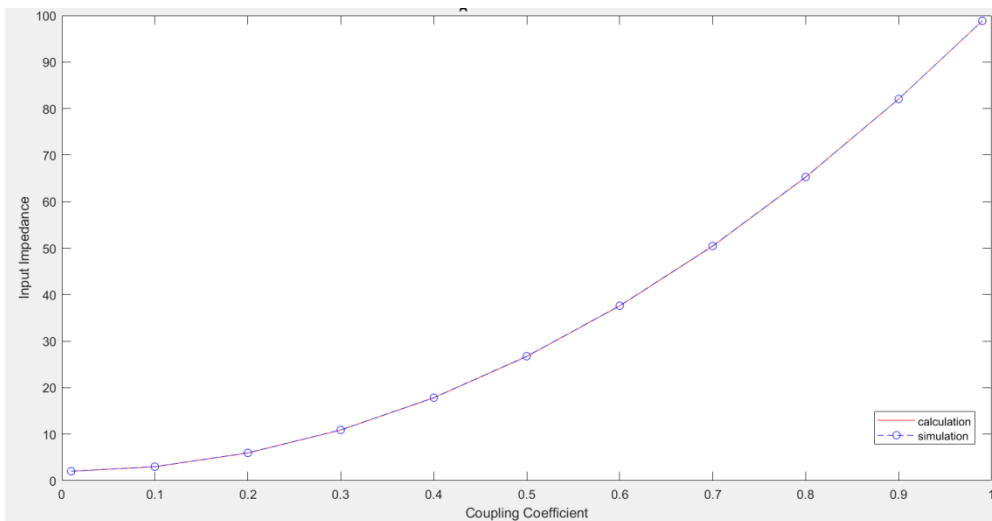


Figure 7: The graph of calculated and simulated input impedance against the coupling coefficient

Finally, the per cent error is plotted for each point of the coupling coefficient as shown in Figure 8. Figure 8 shows that the per cent error is dropped by the increasing of the coupling coefficient. The per cent error is highest at

the lowest coupling coefficient of 0.01. Based on the total per cent error as plotted, the RMS error is also calculated and found to be 0.7999.

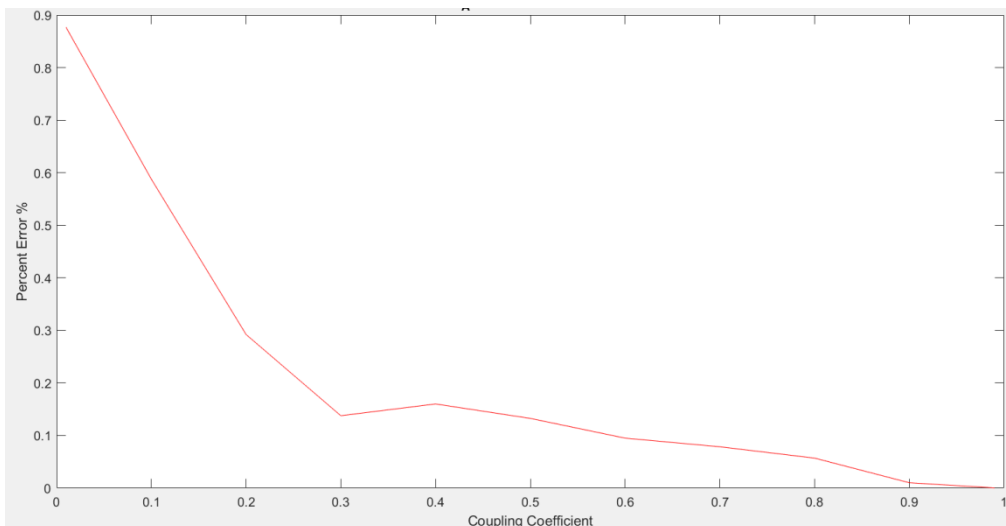


Figure 8: The plot of the per cent error of the calculated and simulated input impedance against the coupling coefficient

The almost linear relationship of the calculated and simulated input impedances with the coupling coefficient has been observed as shown in Figure 7. It provides a way of estimating the coupling coefficient between the two coils [15]. Additionally, the low per cent errors presented in Figure 8 which proves that the input impedance is a reliable coupling coefficient estimating method for two coils.

4. Conclusion

In this paper, the relationship of the input impedance and the coupling coefficient of the series-to-series inductive resonance is analyzed below and above the resonance frequency. The input impedance at the resonance frequency shows an identical relationship in which; the input impedance increased by the coupling coefficient. Further, the relationship between the input impedance and

the coupling coefficient is almost linearly increased. Similarly, the relationship is unique in which each coupling coefficient giving unique input impedance value. Thus, this relationship is easily exploited to estimate the coupling coefficient by giving the input impedance.

The dissimilarity between the calculate and the simulate input impedance is relatively insignificant and can be ignored. From the graph, by comparison, the simulated input impedance is a bit smaller than the calculate input impedance. In addition, the per cent error between the calculated and the simulated data are plotted and analyzed. The plot shows that the per cent error is higher at the lower coupling coefficient and lower at higher coupling coefficient. The lower per cent error suggests higher precision and accuracy. On top, the RMS error is 0.7999 which can be further reduced by system calibration. Anyhow, as the RMS error is very small, it always tolerable. The overall result implies the probability of exploiting the input impedance for the coupling coefficient estimation of the inductive resonant WPT coils. As for an instance, the ability to measure the coupling coefficient of the coils helps in further maximizing the power transfer.

Acknowledgments

We would like to acknowledge the technical and financial assistance by the IIUM Research Management Center (RMC) via (Ref: FRGS/1/2018/TK04/UIAM/02/3), RIGS Grant No RIGS 15-147-0147, and RMC RIGS 16-067-0231

References

- [1] P. Li and R. Bashirullah, "A wireless power interface for rechargeable battery-operated medical implants", *IEEE Trans. Circuits Syst. II, Exp Briefs*, vol. 54, no. 10, pp. 912-916, Oct. 2007.
- [2] R.R. Harrison, "Designing efficient inductive power links for implantable devices", *In: Proc. IEEE Inti. Symposium on Circuits and Systems*, New Orleans, LA, pp. 2080-2083, 2007.
- [3] Chwei-Sen Wang, Oskar H. Stielau, Grant A. Covic, "Design considerations for a contactless Electric Vehicle Battery Charger", *IEEE Transactions on Power Electronics*, vol. 52, no. 5, October 2005.
- [4] A. Kurs, A. Karalis, R. Moffatt, J. D. Joannopoulos, P. Fisher, M. Soljacic, and M. Soljac, "Wireless Power Transfer via Strongly Coupled Magnetic Resonances," *Science* 06 Jul 2007 vol. 317, Issue 5834, pp. 83-86, 2007.
- [5] F. A. Siddiqui, A. Nagani, S. R. Ali, "Wireless Power Transfer Techniques: A Review", *International Journal on Recent and Innovation Trends in Computing and Communication*, vol. 3, issue 12, pp. 6711-6717, 2015.
- [6] I Adam, KA Kadir, Sheroz Khan, A Nurashikin, H Mansor, "Inductive resonant power transfer and topology consideration", *IEEE 3rd International Conference on Engineering Technologies and Social Sciences (ICETSS)*, Aug. 2017.
- [7] C. Nataraj, Sheroz Khan, M. H. Habaebi, and A. G. A. Muthalif, "Resonant Coils Analysis for Inductively Coupled Wireless Power Transfer Applications," *IEEE Int. Instrum. Meas. Technol. Conf.*, no. 1, pp. 109-114, 2016.
- [8] Zhen Chang, K. T. Chau, "Homogeneous Wireless Power Transfer for Move-and-Charge", *IEEE Transactions on Power Electronics*, vol. 30, no. 11, November 2015.
- [9] R. Johari, J. V. Krogmeier, and D. J. Love, "Analysis and practical considerations in implementing multiple transmitters for wireless power transfer via coupled magnetic resonance", *IEEE Trans. Ind. Electron.*, vol. 61, no. 4, pp. 1774-1783, 2014.
- [10] Zhen Chang, K. T. Chau, "Homogeneous Wireless Power Transfer for Move-and-Charge", *IEEE Transactions on Power Electronics*, vol. 30, no. 11, November 2015.
- [11] Qifan Li & Yung C. Lian, "An Inductive Power Transfer System With a High-Q Resonant Tank for Mobile Device Charging", *IEEE Transactions on Power Electronics*, vol. 30, no. 11, November 2015.
- [12] Hongchang Li, Jie Li, Kangping Wang, Wenjie Chen, Xu Yang, "A Maximum Efficiency Point Tracking Control Scheme for Wireless Power Transfer Systems Using Magnetic Resonant Coupling", *IEEE Transactions on Power Electronics*, vol. 30, no. 7, July 2015.
- [13] Su, Y.G.; Zhang, H.Y.; Wang, Z.H.; Hu, A.P.; Chen, L.; Sun, Y. "Steady-State Load Identification Method of Inductive Power Transfer System Based on Switching Capacitors", *IEEE Trans. Power Electron.*, 30, 6349-635., 2015.
- [14] VissutaJiwariyavej, TakchiroImura, Yoichi Hori, "Coupling Coefficients Estimation of Wireless Power Transfer via Magnetic Resonant Coupling Using Information from Either Side of the System", *IEEE Journal of Emerging and Selected Topics in Power Electronics*. vol. 3, no 1, March 2015.
- [15] Sheroz Khan, I. Adam, Z Alam, K F MohdSuhut, N Yusof, "Programmable Solution for Solving Nonlinearity Characteristics of Smart Sensor Applications", *Sensors and Transducers Journal*. vol. 84, 10, 1580-1588., 2007.